SolMech 41st 2018

Development of Non-Contact Fatigue Crack Propagation Monitoring Method Using Air-Coupled Acoustic Emission System

Takuma MATSUO*, Daisuke HATANAKA

School of Science and Technology, Meiji University
1-1-1 Higashi-mita Tama-ku Kawasaki Kanagawa, Japan
*Corresponding Author e-mail: matsuo@meiji.ac.jp

A monitoring system for fatigue crack propagation was developed using a non-contact acoustic emission (AE) monitoring system. The AE signals generated during the plane bending fatigue test were first monitored. The AE generation rate increased after approximately 0.5 of the fatigue life ratio. The maximum amplitude of the AE signals increased with a tendency similar to that of the crack propagation. The sensor sensitivities for the flat and arced surfaces were then compared. The sensitivity improved when the specimen surface was flat. The bar specimen with plane surfaces was used for the AE monitoring of the rotary bending fatigue test. From 0.715 of the fatigue life ratio, the AE generation rate increased after crack generation. The AE signals were detected at an earlier stage of the fatigue life in the flat surface specimen compared with the arc surface specimen during the rotary bending fatigue test. The detection of fatigue cracks in the rotary component at an early stage was possible using a non-contact AE monitoring system.

Key words: acoustic emission; air-coupled ultrasonic sensor; bending fatigue; noise reduction; monitoring.

1. Introduction

Rotating components are commonly used as mechanical components; therefore, the development of a method for the non-destructive monitoring and damage detection in the rotating components at an early stage is required. The acoustic emission (AE) method is an efficient monitoring technique that can be used to assess the integrity of the equipment during operation [1–3]. In particular, the AE method enables the determination of the fatigue crack characteristics using the AE signal analysis [4–10] and can be used to predict the fatigue life of a material [11–16]. However, the fatigue monitoring of rotating components during operation is difficult because the attachment of a sensor to the surface of the rotating component is difficult [17–19]. To overcome this problem, a non-contact

AE monitoring system was developed and used for the fatigue monitoring of rotating components in our group [20]. This system utilizes an air-coupled ultrasonic sensor to detect the AE signals and improves the signal-to-noise (SN) ratio of the signals by reducing the noise in real time using the noise reduction function of the AE monitoring system. In a previous study, the AE was assumed to be generated by the contact of cracked surfaces [21]. The AE signals from the crack initiation and propagation at an early stage were not detected, even though the AE signals were detected immediately before the fracture.

The purpose of this study is to develop a method for fatigue crack monitoring using the developed non-contact AE monitoring system. We first compared the timings of the AE generation of the plane bending and bending fatigue tests in the rotating component. We next determined the relationship between the sensor sensitivity and surface condition of the specimen. Finally, the AE signals from the bending fatigue test in the rotating component was monitored using a modified specimen using the developed system.

2. AE MONITORING DURING PLANE BENDING FATIGUE TEST

The AE signals were monitored during a plane bending fatigue test using the non-contact AE monitoring system. Figure 1 shows the experimental setup for monitoring the AE signals during a plane bending fatigue test. The AE monitoring system was composed of an air-coupled ultrasonic sensor (The Ultran Group: NCG200-D25, resonant frequency: 200 kHz) and a digitizer with the noise reduction function [22]. The trigger level of the AE detection was 10 mV. The bending loading frequency, stress amplitude, and stress ratio were 5 Hz, $\sigma_a = 134$ MPa and $R = -0.72$, respectively. The air-coupled ultrasonic sensor was positioned over the surface of the specimen at a distance of 5 mm. The
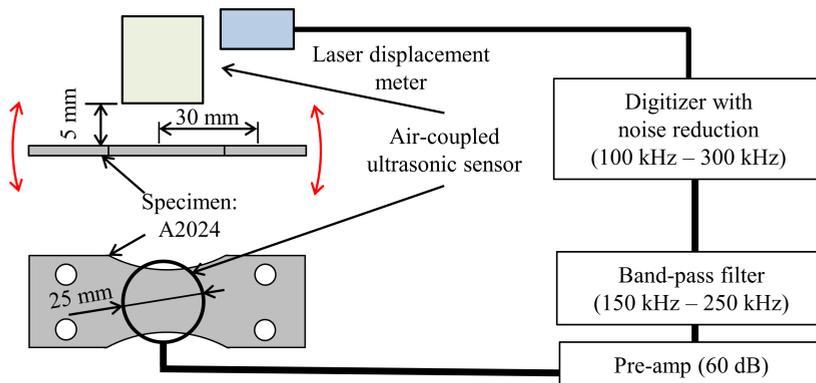

FIG. 1. Experimental setup for monitoring the AE signals during the plane bending fatigue test.

laser displacement sensor was set 30 mm above the surface of the specimen to monitor the stress processes of the specimen. Figure 2 shows the specimen for a plane bending fatigue test. The specimen material was A2024 with a thickness of 4 mm. Both ends of the specimen mid-section contained slits of width 1 mm and length 1 mm, to limit crack initiation locations. A mirror finished surface for the specimen was used to easily observe the fatigue cracks. The fatigue crack lengths on the surface of the specimen were measured by the replica method. The plane bending fatigue test machine was stopping during application of the replica method. The surface of the specimen experienced tensile stress to open cracks.
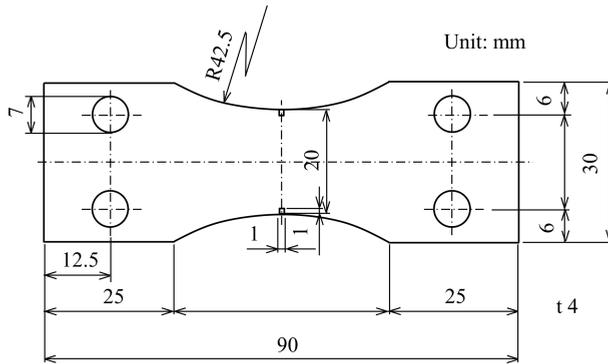
Fig. 2. Configuration of the specimen for the plane bending fatigue test.

The specimen was fractured at approximately 27.9 ks. Figure 3 shows the cumulative AE events during the plane bending fatigue test. The number of
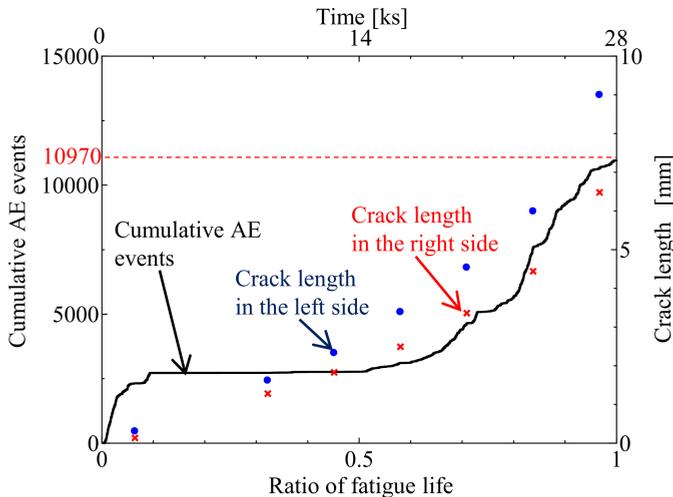
Fig. 3. Change in cumulative AE events during the plane bending fatigue test and crack observations.

detected AE signals was 10970 events. AE signals were continuously detected from the test initiation to approximately 0.1 of the fatigue life ratio. The AE signals were generated by the plastic deformation of the contact surface between the specimen and jigs, after which, only insignificant AE signals were detected. From greater than 0.5 of the fatigue life ratio, the AE generation rate gradually increased. It was estimated that the fatigue cracks started to emitted AE signals. From this time to the final fracture of the specimen, AE signals were continuously detected. In Fig. 3, the blue and red points show the crack lengths of the left and right sides of the specimen, respectively. The fatigue crack on the left side propagated faster than the right side. Moreover, the fatigue cracks exponentially increased during the plane bending fatigue test.

Figure 4 shows the maximum amplitude distribution of the AE signals during the plane bending fatigue test. For fatigue life ratio greater than approximately 0.4 until the final fracture of the specimen, the maximum amplitude of the AE signals increased with a similar tendency to that of the crack propagation. The maximum amplitude of the AE signals increased because the crack growth rate increased. From this result, it was assumed that the detected AE signals were generated by the crack propagation.
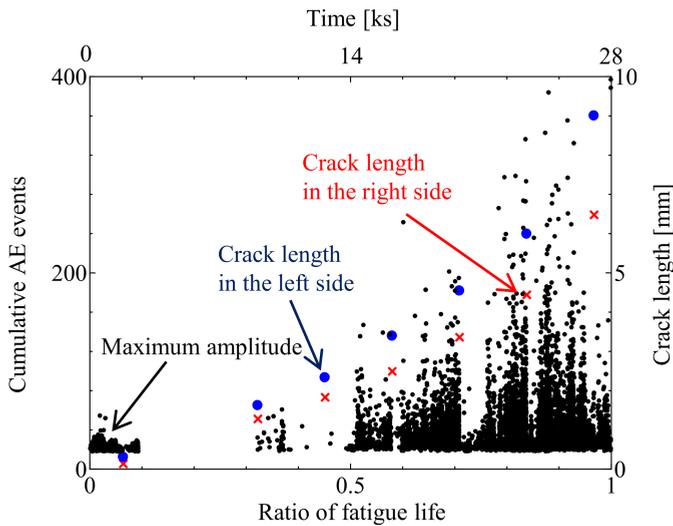

Fig. 4. Changes in the maximum amplitude during the plane bending fatigue test and crack observations.

The relationship between the state of the specimen under applied stress and the AE generation timing were also considered. Figure 5 shows the state of the specimen for each stress phase. The 0° phase represents the case for which no stress is applied to the specimen surface. The 90 and 270° phases represent the
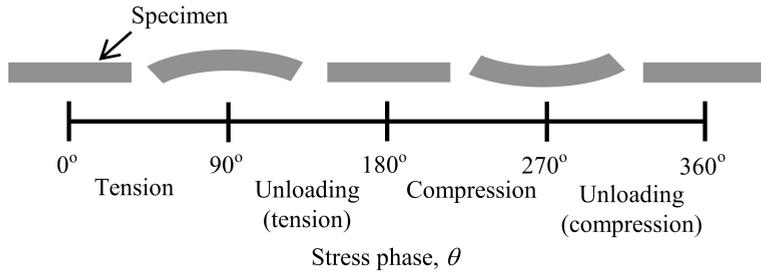
FIG. 5. Relationship between the stress phase and state of the specimen.

maximum tensile and maximum compressive stresses applied to the specimen surface, respectively. The applied stress processes were: tension for $0° \leq \theta < 90°$, unloading of tension for $90° \leq \theta < 180°$, compression for $180° \leq \theta < 270°$, and unloading of compression for $270° \leq \theta < 360°$.

Figure 6 shows the relationship between the stress phase and AE generation timing. From the test initiation to approximately 0.1 of the fatigue life ratio, the AE signals were detected for $200° \leq \theta < 270°$. The AE signals were generated by the plastic deformation of the contact surface between the specimen and jigs. From approximately 0.5 of the fatigue life ratio to the final fracture of the specimen, the AE signals were detected for $0° \leq \theta < 90°$. The AE signals were generated by the crack generation and propagation. From this time, the cumulative AE events increased. From approximately 0.6 of fatigue life ratio to the final fracture of the specimen, the AE signals were detected for $90° \leq \theta < 135°$. These AE signals were generated by the contact of the cracked surface due to
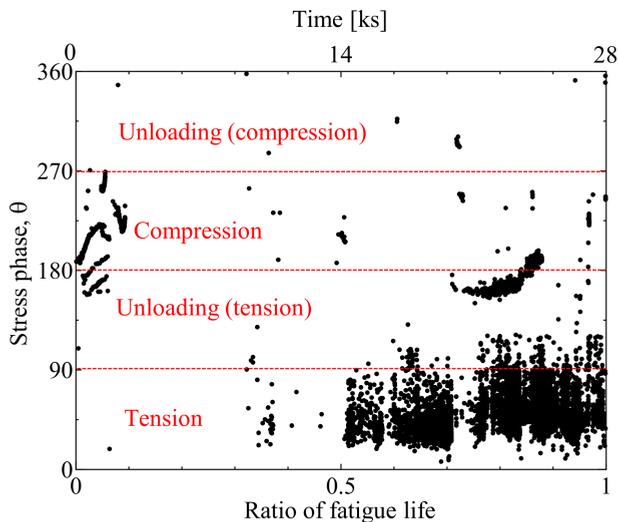

FIG. 6. Relationship between the stress phase and AE generation timing.

close cracks. From approximately 0.7 to 0.9 of fatigue life ratio, the AE signals were detected for $135° \leq \theta < 225°$. These AE signals were generated by damage of the fractured surface due to the applied compressive stress. From these results, it was estimated that the AE signals were generated by the crack generation and propagation and contact of the crack surface.

Figure 7 shows the AE waveform detected at a) 0.013, b) 0.577, and c) 0.860 of the fatigue life ratio, and (d) the final fracture. For the AE waveform detected at 0.013 of the fatigue life ratio, it was assumed that plastic formation or friction of the jigs occurred. The AE waveforms detected at 0.577 and 0.860 of the fatigue life ratio were generated by the propagation of cracks because the AE waveforms were detected at $\theta = 60$ and $64°$, respectively. The amplitude of the
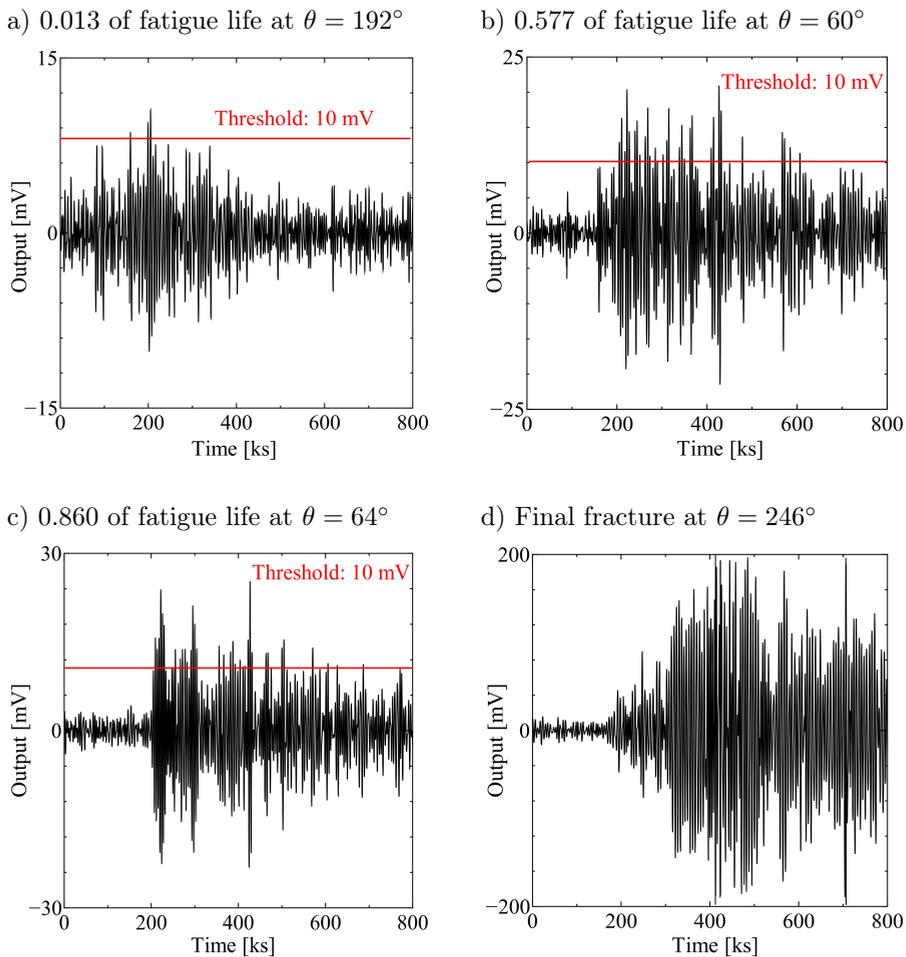

FIG. 7. AE waveforms detected at (a) 0.013, (b) 0.557, and (c) 0.860 of the fatigue life ratio and (d) the final fracture.

AE waveform detected for the final fracture was highest of all the AE waveforms during the test.

Figure 8 shows the fracture surface after the plane bending fatigue tests. In Fig. 8(a), the blue lines show the crack length at 0.580 of the fatigue life ratio, and after this time, a black surface was formed on the fracture surface, as shown in Fig. 8(b). The black surface was formed by the adhesion of the abrasion powder that was generated by the fretting between the fracture surfaces [23, 24]. From 0.580 of the fatigue life ratio, AE signals were detected during the unloading of the tension and compression processes. From this result, it was assumed that the AE signals were generated by crack propagation and the contact of the fracture surfaces after this time. Striation was observed at the center of the fracture surface shown in Fig. 8(c). The striation is evidence that the specimen was fractured by fatigue [25]. Thus, the initiation and propagation of fatigue cracks could be monitored by the developed non-contact AE monitoring system.
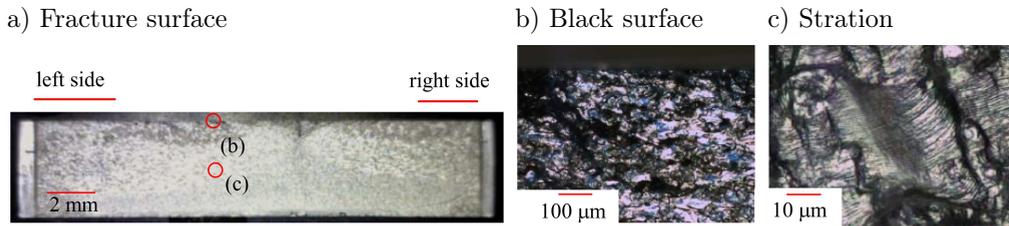
a) Fracture surface   b) Black surface   c) Stration

FIG. 8. Fracture surface after the plane bending fatigue test with a crack length at 0.580 of the fatigue life ratio.

3. RELATIONSHIP BETWEEN THE SURFACE SHAPE OF THE SPECIMEN AND SENSITIVITY OF THE SYSTEM

Fatigue monitoring of aluminum plates is possible by using the developed non-contact AE monitoring system. However, this result was different to a previous study of the bending fatigue test of the rotation of a circular bar [13]. In the previous test, AE signals were only detected just before the final fracture. To overcome this problem, the relationship between the sensitivity of the AE signals detected by the system and configuration of the specimen during the test was investigated. The amplitude of the artificial AE signals propagating in the arc and flat surface specimen were compared. Figure 9 shows the experimental setup for comparing the plane and arc surfaces. The arc surface specimen was a rod of diameter 18 mm. The flat surface specimen was machined by milling a cylinder of diameter 18 mm on the upper side at a depth of 4 mm and length of 25 mm. The air coupled ultrasonic sensor used for the detection of the AE signal was position on top of the surface at a distance of 20 mm. The artificial AE was generated
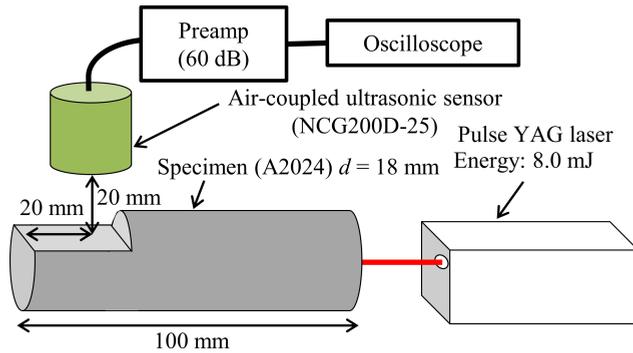
Fig. 9. Experimental setup for comparing the sensitivity of the air-coupled ultrasonic sensor on top of arc and flat surfaces.

by a pulse YAG laser at 8.0 mJ on the end surface of the specimen. Figure 10 shows the waveforms generated by the pulse YAG laser on the (a) arc specimen and (b) arc specimen with a flat surface. The SN ratio of the signals in the arc and flat surfaces were 26.3 and 38.4 dB, respectively. This result indicated that the SN ratio of the AE signals was dependent on the specimen configuration. It was necessary to consider the configuration of the specimen used in the rotary bending fatigue test to detect the AE signals at an early stage.
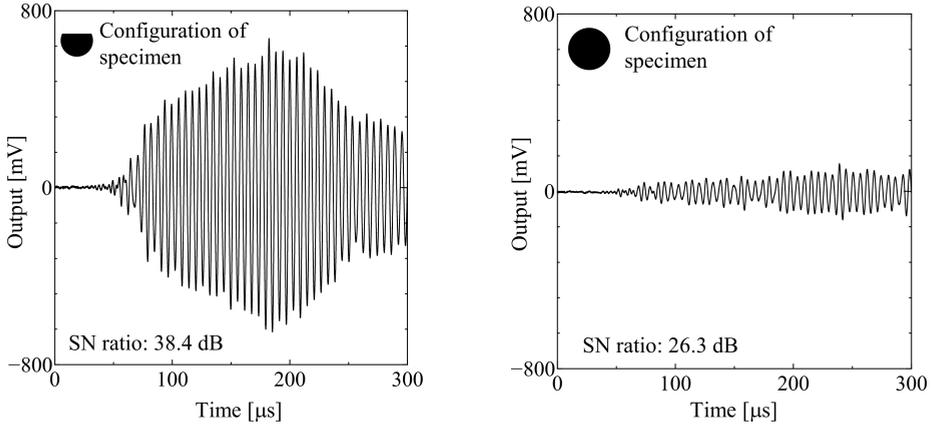

Fig. 10. Waveforms detected by the air-coupled ultrasonic sensor for the arc (right) and flat (left) surface specimens.

4. AE monitoring during the rotary bending fatigue test using the circular bar specimen with a flat surface

The result in the previous chapter indicated that the plane surface shape had a greater efficiency than that of the arc surface shape using the air-coupled

ultrasonic sensor. Therefore, the circular bar specimen with a flat surface for the rotary bending fatigue test was machined and utilized for fatigue monitoring. Figures 11 and 12 show the specimen configuration and experimental setup, respectively. The specimen was an aluminum alloy (A2024) with 18 mm diameter and 120 mm length. The flat surface was made by milling a cylinder of diameter 18 mm on the upper and under sides at a depth of 4 mm and length of 25 mm. A slit of 0.5 mm depth and 1 mm width was made on the end of the flat surface to limit crack initiation. The surface of the specimen was mirror finished so that it was easy to observe the fatigue cracks. The fatigue crack lengths on the surface of the specimen were measured by the replica method. The loading frequency was 3 Hz, and the load was 294 N. The air-coupled ultrasonic sensor was positioned on top of the surface of the specimen. The detected AE signals were amplified by 60 dB using a pre-amplifier. The passband was from 150 to 250 kHz with a trigger level of 7 mV. The air-coupled ultrasonic sensor was setup as for the test with the flat surface specimen.
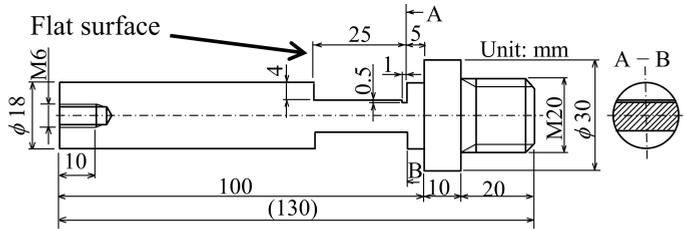

FIG. 11. Configuration of the specimen for the rotary bending fatigue test.
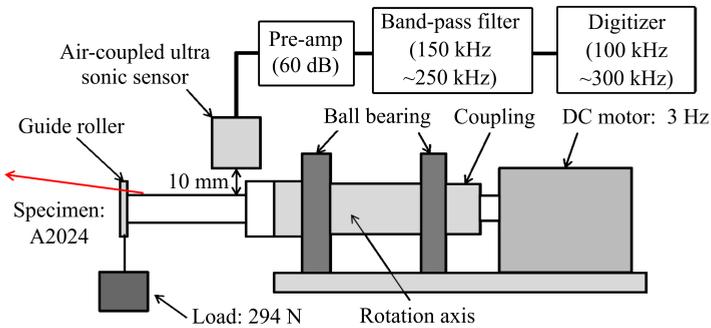

FIG. 12. Experimental setup for monitoring the AE signals during the rotary bending fatigue test.

The specimen was fractured at approximately 172 ks. Figure 13 shows the cumulative AE events during the test, and crack lengths in the specimen. The number of detected AE signals was 318 events. The fatigue crack was confirmed at 0.710 of the fatigue life ratio on the left side, and the cracks exponentially in-
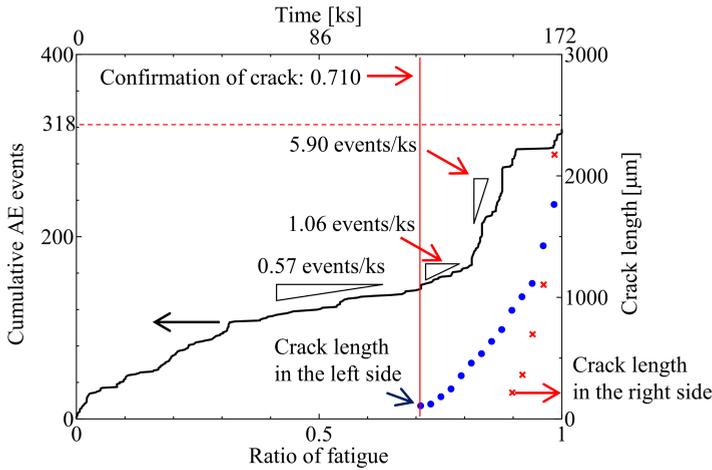
FIG. 13. Cumulative AE events and crack lengths in both sides of the specimen.

creased during the rotary bending fatigue test. From the test initiation, AE signals were continuously generated. The AE signals before the confirmation of cracks were noise generated by the test machine. From 0.710 of the fatigue life ratio, the AE generation rate increased near the same time. From 0.815 to 0.919 of the fatigue life ratio, the AE generation rate rapidly increased again. Figure 14 shows the AE waveforms detected at (a) 0.049 and (b) 0.898 of the fatigue life ratio. The AE waveform detected at 0.049 of fatigue life ratio was detected before the generation of cracks. This AE waveform was generated by the testing machine or the plastic deformation of the specimen. The AE waveform detected at 0.898 of the fatigue life ratio was detected at the same time as the increasing AE generation rate.
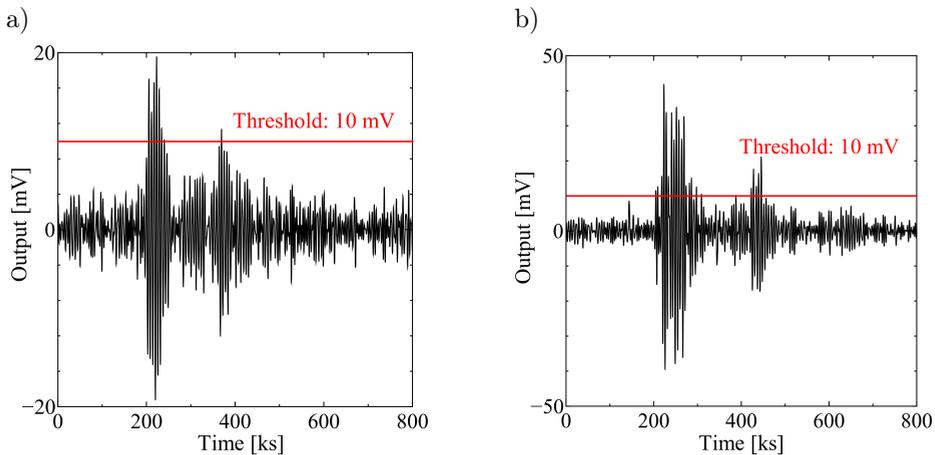

FIG. 14. AE waveforms detected at (a) 0.049 and (b) 0.815 of the fatigue life ratio.

Figure 15 shows the maximum amplitudes of AE signals during the plane bending fatigue test. From the test initiation to approximately 0.7 of the fatigue life ratio, the maximum amplitude of the AE signals decreased with time. From approximately 0.7 of the fatigue life ratio, the maximum amplitude of the AE signals increased. In particular, the AE signals whose maximum amplitude was greater than that at other times were detected at 0.815 of the fatigue life ratio. These AE signals were generated by crack propagation. The AE signals were detected again at 0.985 of the fatigue life ratio, and the maximum amplitude of the AE signals increased until the final fracture. This result was similar to the results of the plane bending fatigue test, and the fatigue crack propagation was roughly related to the AE amplitude.
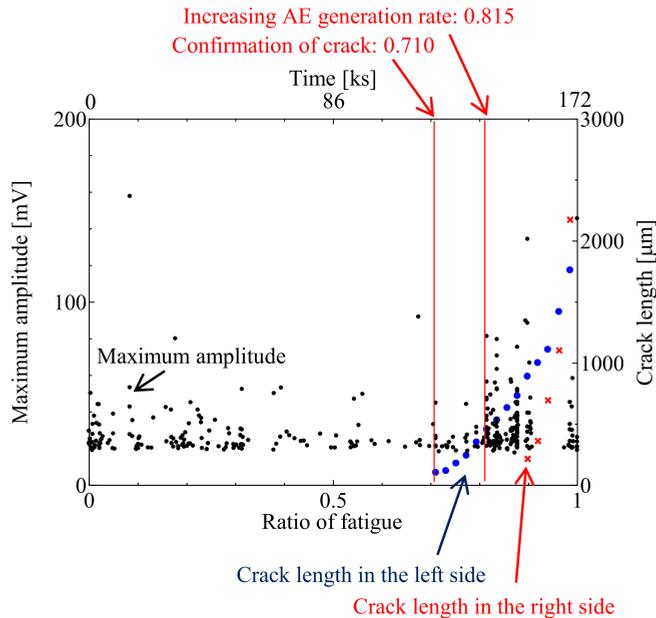

Fig. 15. Change in the maximum amplitude during the rotary bending fatigue test using the flat surface specimen, and the crack observations.

Figure 16 shows the fracture surface after the rotary bending fatigue test. Figure 16a shows the general view of the fracture surface. The cracks were generated at the corner of the flat surface, and propagated from the corner to the center of its cross section, before the specimen was fractured. Figure 16b shows the part of the fracture surface that turned black. Figure 16c shows the cracked surface. Figure 16d shows the striation in the fracture surface. The fatigue crack propagation corresponded to the AE generation rate. In addition, the detection of the fatigue crack in the rotary component at an early stage is possible by a non-contact AE system using a specimen with flat surfaces.

a) Fracture surface   b) Black surface

Rotating direction

2 mm

c) Crack surface   d) Striation

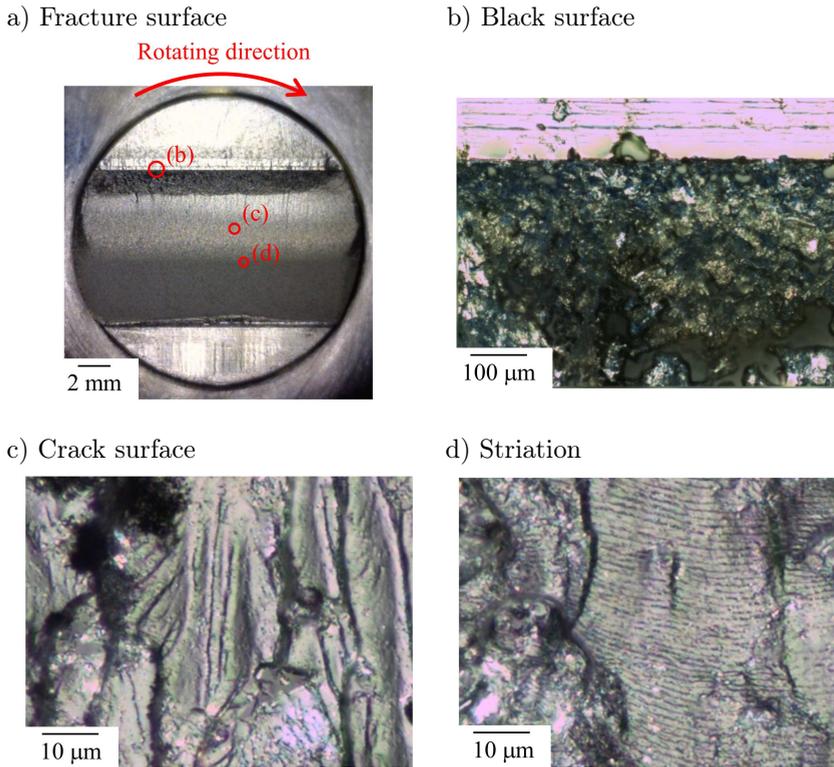10 μm   10 μm

FIG. 16. Fracture surface after the rotary bending fatigue test using the specimen with a flat surface.

5. CONCLUSION

A non-contact AE monitoring system was used to detect AE signals during rotary bending fatigue tests. The AE signals were detected at an early stage of fatigue during the test. The results are given below:

1) The AE signals were detected at an earlier stage of fatigue compared with the rotary bending fatigue test during the plane bending fatigue test. These AE signals were assumed to be caused by the crack propagation and contact of fracture surfaces.

2) The sensitivities of the sensor for flat and arc surfaces were compared. The sensitivity improved by about 12 dB when the specimen surface was flat.

3) The AE signals were detected at an earlier stage of the fatigue life for the flat surface specimen compared with the arc surface specimen during the rotary bending fatigue test. The detection of fatigue cracks at an earlier stage is possible by the non-contact AE monitoring system.

References

1. Mizutani Y., *Practical acoustic emission testing*, Springer, Berlin 2006.

2. Grosse C.U., Ohtsu M., *Acoustic emission testing*, Springer, Berlin 2008.

3. Eftekharnejad B., Addali A., Mba D., *Shaft crack diagnostics in a gearbox*, Applied Acoustics, **73**: 723–733, 2012.

4. Roberts T.M., Talebzadeh M., *Acoustic emission monitoring of fatigue crack propagation*, Journal of Constructional Steel Research, **59**: 695–712, 2003.

5. Berkovits A., Fang D., *Study of fatigue crack characteristics by acoustic emission*, Engineering Fracture Mechanics, **51**: 401–416, 1995.

6. Lindley T.C., Palmer I.G., Richards C.E., *Acoustic emission monitoring of fatigue crack growth*, Materials Science and Engineering, **32**: 1–15, 1978.

7. Aggelis D.G., Kordatos E.Z., Matikas T.E., *Acoustic emission for fatigue damage characterization in metal plates*, Mechanics Research Communications, **38**: 106–110, 2011.

8. Scala C.M., Cousland S.M., *Acoustic emission during fatigue crack propagation in the aluminum alloys 2024 and 2124*, Material Science and Engineering, **61**: 211–218, 1983.

9. Morton T.M., Harrington R.M., Bjeletich J.G., *Acoustic emission of fatigue crack growth*, Engineering Fracture Mechanics, **5**: 691–697, 1973.

10. Sinclair A.C.E., Connors D.C., *Acoustic emission analysis during fatigue crack growth in steel*, Materials Science and Engineering, **28**: 263–273, 1977.

11. Jianguo Y., Ziehl P., Zarate B., Caicedo J., *Prediction of fatigue crack growth in steel bridge components using acoustic emission*, Journal of Constructional Steel Research, **67**: 1254–1260, 2011.

12. Roberts T.M., Talebzadeh M., *Fatigue life prediction based on crack propagation and acoustic emission count rates*, Journal of Constructional Steel Research, **59**: 679–694, 2003.

13. Whitlow T., Sundaresan M., *Clustering of Fiber-break related events in carbon fiber reinforced polymer composites using acoustic emission*, Journal of Acoustic Emission, **34**: 52–63, 2017.

14. Bhuiyan M.Y., Lin B., Giurgiutiu V., *Acoustic emission sensor effect and waveform evolution during fatigue crack growth in thin metallic plate*, Journal of Intelligent Material Systems and Structures, **29**: 1275–1284, 2018.

15. Deschanel S., Rhouma W.B., Weiss J., *Acoustic emission multiples as early warnings of fatigue failure in metallic materials*, Scientific Reports, **7**: 13680, 10 pages, 2017.

16. Chai M., Duan Q., Hou X., Zhang Z., Li L., *Fracture toughness evaluation of 316LN stainless steel and weld using acoustic emission technique*, ISIJ International, **56**: 875–882, 2016.

17. Liu J., Shi Z., Shao Y., *An investigation of a detection method for a subsurface crack in the outer race of a cylindrical roller bearing*, Maintenance and Reliability, **19**: 211–219, 2017.

18. Holford K.M., Eaton M.J., Hensman J.J., Pullin R., Evans S.L., Dervilis N., Worden K., *A new methodology for automating acoustic emission detection of metallic*

fatigue fractures in highly demanding aerospace environments: An overview, Progress in Aerospace Sciences, **90**: 1–11, 2017.

19. NISHINA Y., IMANISHI D., *Basic study on crack diagnosis of rotary equipment by fluid-mediated AE method*, mechanical Engineering Journal, **4**: 16-00406, 7 pages, 2017.

20. OTA Y., MATSUO T., CHO H., *Detection of bending fatigue in a rotating component utilizing a non-contact AE monitoring system*, Proceedings of the 2012 M&M Symposium for Young Researchers, 2012.

21. MATSUO T., CHO H., *Development of AE monitoring system with noise reduction function by spectral subtraction*, Materials Transactions, **53**: 342–348, 2012.

22. HATANAKA D., MATSUO T., *Estimation of AE generation mechanisms in rotating components during fatigue test* [in Japanese], Progress in Acoustic Emission, pp. 109–112, 2015.

23. TOKAJI K., OGAWA T., KATO Y., *Static strength and rotating bending fatigue strength of aluminum-lithium alloys* [in Japanese], Journal of the Society of Materials Science, **39**: 64–69, 1990.

24. YAMABE J., KOBAYASHI M., *Effect of hardness and stress ratio on threshold stress intensity factor ranges for small cracks and long cracks* [in Japanese], Transactions of the Japan Society of Mechanical Engineers, **71**: 88–96, 2005.

25. SURESH S., *Fatigue of materials*, 2nd ed., Cambridge University Press, Cambridge 1998.